Journal of Physics:
Conference Series

PAPER • OPEN ACCESS

On UAV Terrestrial Connectivity Enhancement through Smart Selective Antennas

To cite this article: Emanuele Pagliari *et al* 2024 *J. Phys.: Conf. Ser.* **2716** 012057

On UAV Terrestrial Connectivity Enhancement through Smart Selective Antennas

Emanuele Pagliari[1], Luca Davoli[1], Giordano Cicioni[2], Valentina Palazzi[2], and Gianluigi Ferrari[1]

[1] Internet of Things (IoT) Lab, Department of Engineering and Architecture, University of Parma, Italy, and National Inter-University Consortium for Telecommunications (CNIT), Parma, Italy.

[2] Department of Engineering, University of Perugia, Italy

E-mail: `emanuele.pagliari@unipr.it`, `luca.davoli@unipr.it`, `giordano.cicioni@studenti.unipg.it`, `valentina.palazzi@unipg.it`, `gianluigi.ferrari@unipr.it`

Abstract. Nowadays, Unmanned Aerial Vehicles (UAVs) are widely used in heterogeneous contexts and, thanks to a continuous technological evolution, are going to be used for several applications such as, for example, Beyond Visual Line of Sight (BVLOS) operations. Since in BVLOS flights the UAV and the ground control center may not have a direct visibility with each other, a robust communication system is needed to provide reliable connectivity. Although a cellular (4G/5G) network is the current best candidate to enable BVLOS applications, there are still some limitations to overcome, as 4G (LTE) and 5G (NR) cellular networks are natively designed for terrestrial use. In this paper, we *first* investigate current cellular communication limitations for UAV-based applications, in particular taking into account both results available in the literature, as well as experimental performance campaigns. *Then*, a viable solution for mitigating these drawbacks exploiting selective *on-board* antennas is proposed, whose performance is experimentally investigated with a preliminary prototypical architecture.

1. Introduction

In the last decade, the UAV market sector has experienced a steady growth and is expected to further expand by 2030 [1], also thanks to UAV adoption in several heterogeneous scenarios, such as surveillance, rescue operations in harsh environments, environmental monitoring, experimental delivery services, and so on. However, due to regulations and technical limitations, so far most of the applications have been mainly carried out in Visual Line of Sight (VLOS) conditions, where existing solutions are reliable and effective. Although VLOS flights still have significant growth opportunities, most of the drone manufacturing companies are nowadays targeting the adoption of UAVs in Beyond VLOS (BVLOS) scenarios, in order to enable complex missions and advanced services over large areas.

A key technical challenge of BVLOS applications is network connectivity, for both Command and Control (C2) and application-related data exchange. Illustrative examples include real-time video feeds kept from *on-board* cameras, data collection from Internet of Things (IoT) sensing nodes deployed in the surrounding environment, and connectivity provision to ground devices located in the area where the UAV is flying over. Therefore, strong and reliable bi-directional communication links are needed in these BVLOS-like scenarios. Commercial UAV

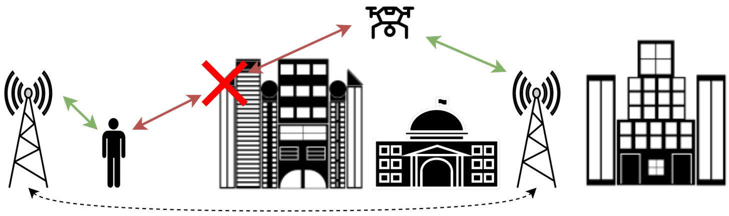

Figure 1: Generic cellular connectivity-enabled UAV BVLOS scenario.

manufactures have investigated the use of existing cellular networks for BVLOS missions, leading to the implementation of high-end quad-copters exploiting cellular communications [2] to extend their flight missions' operating range, as graphically shown in Figure 1.

As of now, canonical UAVs use 4G LTE connectivity only as a backup solution in case of failure of traditional *point-to-point* wireless communication links between the drone and the pilot. This is because, despite a widespread adoption of cellular networks for terrestrial applications (whose maturity and reliability are clear), the adoption of the same paradigms for aerial applications still needs to be thoroughly investigated, since currently deployed cellular networks are optimized for terrestrial use. In fact, cellular deployment and frequency reuse plans between nearby cells have been optimized to avoid inter-cell interference on ground-located connected terminals. However, since UAVs can fly at several altitudes (with the most common commercial drones typically flying close to a 100 m Above Ground Level, AGL, altitude), a cellular terminal located on a drone will be in direct visibility with multiple Base Transceiver Stations (BTSs) of nearby cells, especially in geographically flat environments or in high population density regions (where several BTSs are deployed in a limited region). This leads to a strong inter-cell interference, since a UAV receives strong signals from the neighboring BTSs, whose detrimental effects have been experimentally verified through *in-flights* cellular network signal measurements carried out by several entities (i.e., Internet Service Providers, ISPs, and research institutions). Consequently, a degradation of radio signal quality metrics is observed, eventually affecting the network effective performance and stability, thus limiting the safety of critical BVLOS missions.

In this paper, we *first* investigate the current cellular connectivity drawbacks for UAV applications identified in the literature (together with already provided solutions). *Then*, we propose and detail a prototypical antenna architecture composed by a selective antenna system useful to mitigate the inter-cell interference issue. *Finally*, we provide some preliminary experimental performance results based on well-known 4G LTE radio quality indexes and the number of cell changes, evaluated at different flight altitudes.

The paper is organized as follows. In Section 2, a literature overview on UAV-oriented cellular connectivity is presented, analyzing limitations and possible solutions. Section 3 presents our prototypical architecture featuring a smart selective antenna system, while in Section 4 some preliminary experimental results are shown. Finally, an overall discussion, together with improvements and future research directions, is provided in Section 5.

2. Related Works

According to well-known cellular network vendors [3,4] (and as will be experimentally investigated in Section 4 with regard to the behaviour of 4G LTE cellular networks signals quality indexes at different flight altitudes), it has been shown that, depending on the environment morphology and BTSs' spatial density, at 100 m AGL flight height the free-space path loss propagation of radio signals transmitted by nearby 4G LTE BTSs has a relevant impact on UAV connectivity, thus hindering the overall network stability.

In [3–6], it is confirmed that current cellular network implementations are not optimized for aerial utilization. Therefore, even if they are already used for backup and non-critical UAV connectivity applications, several drawbacks and issues are still to overcome to assure sufficient reliability, especially for critical BVLOS missions. For the sake of completeness, a similar behaviour has been observed through our experimental *in-flight* measurements performed in a semi-rural area in the north of Italy at different flight heights (from ground level up to 120 m AGL) using a traditional omni-directional 4G LTE antenna on the UAV. The following four most relevant 4G LTE radio signal quality indexes (as defined by the 3GPP [7]) have been evaluated.

- The Received Signal Strength Indicator (RSSI, dimension: [mW]) is the pure wide band measured power, depending on the connected cell signal as well as interfering signals from nearby cells and thermal noise. The RSSI can be expressed as

$$\mathrm{RSSI} = S_{\mathrm{tot}} + I_{\mathrm{tot}} + N_{\mathrm{tot}} \tag{1}$$

  where: S_{tot} (dimension: [mW]) is the useful received signal power; I_{tot} (dimension: [mW]) and N_{tot} (dimension: [mW]) are the interference and thermal noise powers, respectively. All powers are measured over the 12 Resource Elements (REs) subcarriers foreseen in the 4G standard [7].

- The Reference Signals Received Power (RSRP, dimension: [mW]) indicates the useful received signal power of the connected BTS and can be expressed as

$$\mathrm{RSRP} = \frac{1}{N_{\mathrm{RE}}} \sum_{i=1}^{N_{\mathrm{RE}}} P_{r,i} \tag{2}$$

  where: N_{RE} is the number of usable REs within the measurement frequency bandwidth, and $P_{r,i}$ (dimension: [mW]) is the power contribution of the i-th RE.

- The Reference Signal Received Quality (RSRQ, adimensional) is used to assess the overall quality of the received signals, thus allowing to decide which cell to connect to, and can be expressed as

$$\mathrm{RSRQ} = \frac{N_{\mathrm{PRB}} \cdot \mathrm{RSRP}}{\mathrm{RSSI}} \tag{3}$$

  where N_{PRB} is the number of Physical Resource Blocks (PRBs).

- The Signal-to-Interference-plus-Noise Ratio (SINR, adimensional) quantifies the relative strength of the useful signal (with respect to noise), and can be expressed as

$$\mathrm{SINR} = \frac{1}{\frac{1}{12 \cdot \mathrm{RSRQ}} - \frac{N_{\mathrm{RE}}}{N_{\mathrm{PRB_{used}}}}} \tag{4}$$

  where: N_{RE} and $N_{\mathrm{PRB_{used}}}$ correspond to the numbers of REs and used PRBs within the measurement band, respectively; and 12 is the number of REs' subcarriers.

For a better comparison, in the following the logarithmic scale is adopted: therefore, SINR and RSRQ are expressed in dB, while RSSI and RSRP in dBm. The obtained results are shown in Figure 2: it can be noticed, for increasing altitude, that SINR and RSRQ reduce (Figure 2(a)) while RSSI and RSRP increase (Figure 2(b)).

On the basis of observed performance, several approaches have been investigated to improve the integration of 4G LTE cellular connectivity for UAV applications: (i) optimizing the existing cellular networks to extend their coverage for aerial devices; (ii) optimizing the flight path of cellular connected UAVs; (iii) using selective antennas on the drones. With regard to the *first* approach, the 3rd Generation Partnership Project (3GPP) Release 15 [8] introduced enhancements aiming at mitigating the interference problem [9]. However, despite various

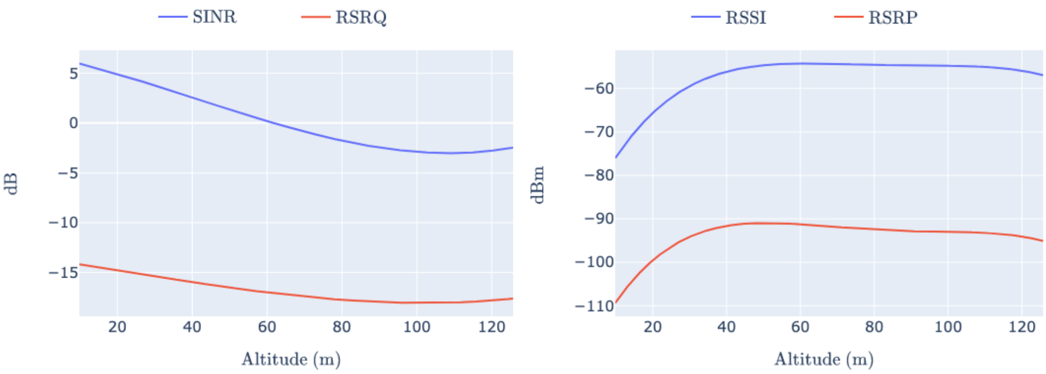

(a) (b)

Figure 2: Omni-directional antennas signal quality metrics different altitudes, in terms of (a) SINR and RSRQ, and (b) RSRP and RSSI.

technical studies and mitigation approaches, the assumptions, models, and techniques used in the design and deployment of 4G cellular networks need to be revisited: this can be partially carried out with 5G and, hopefully, with 6G. The *second* approach has been evaluated in the literature in [10], where the UAV's flight path is planned according to the cellular radio signal quality, targeting a route optimization to ensure a reliable connectivity. However, this approach requires the definition of a radio map based on several field measurements and cannot always be applied, since, for specific flight missions, a flight path's change is not possible. Finally, the *third* approach has been investigated in [11] through a novel theoretical model for aerial 4G LTE cellular connectivity. Promising results have been obtained, through simulations, on the use of directive antennas located on the UAV: however, a validation in real testbeds is still missing.

Given the feasibility of adopting selective antennas on a drone and since this solution enables UAVs to exploit existing cellular networks without modifying the radio equipment's mounted on thousands of cell towers, in this paper we focus on the design and development of a novel prototypical communication architecture including four selective antennas mounted on the drone and controlled by a proper algorithm, aiming at enhancing the UAV's connectivity reliability with the existing 4G LTE networks in BVLOS scenarios.

3. Proposed Selective Antenna System

The proposed prototype is composed by four antennas, connected to the cellular modem on board the drone by means of a network switch. In particular, only the antenna pointing in the direction of the BTS (out of all the antennas) is activated at a time, to reduce inter-cell interference arriving from other nearby BTSs. The active antenna is selected on the basis of drone's and cell towers' relative positions, obtained through the UAV's Flight Controller (FC) and via an *a-priori* access to open-data lists of BTSs, respectively.

More in detail, the antenna system, shown in Figure 3(a), features four directional antennas, mounted on a square support attached to the UAV platform, providing a 360° radio coverage on the horizontal plane. The antennas have been designed in planar technology, as grounded stacked V-slotted patches, to operate in vertical polarization on existing 4G LTE cellular networks—within a frequency range from 1800 MHz (LTE Band 3: 1710 ÷ 1880 MHz) up to 2690 MHz (LTE Band 7: 2500 ÷ 2690 MHz). Each antenna consists of 2 elements aligned horizontally, at a 10 cm distance, so that, including the 3D-printed frame, each antenna has a $21 \times 11 \times 2.4$ cm size and weighs 153 g. In the operational frequency range, the single antenna element has a horizontal 3 dB beamwidth on the H-plane between 60° and 80°, and a vertical 3 dB beamwidth

(a) (b)

Figure 3: (a) Block diagram of the selective antenna system, where the sectors are selected one at a time, and (b) prototypical selective antenna system mounted on the reference UAV.

(E-plane) between 56° and 65°.

The antennas are connected to a custom network switch, consisting of a pair of Single-Pole 4-Throw (SP4T) commercial radio-frequency switches, one per channel, and controlled by a Raspberry Pi 4 (RPi4) Single Board Computer (SBC), that is powered by the UAV's battery and connected to the drone's FC to retrieve the main telemetry data. The 4G cellular modem located on board the drone is a Sierra Wireless EM9191 [12], equipped with coaxial ports to connect to the network switch. The complete system—four antennas, network switch, RPi4, EM9191 cellular modem, and coaxial cables—has a final payload weight of about 1.1 kg.

The selective antenna system has been integrated in a custom-built quad-copter, as shown in Figure 3(b), where the four antennas are shifted by 45° with respect to the drone's front, to avoid potential interference introduced by the carbon fiber legs of the UAV.

Regarding the algorithms defined for controlling the proposed antenna system, two real-time mechanisms have been defined and used for *in-flight* data collection: (i) "nearest BTS" (NBTS) selection algorithm and (ii) "connected BTS" (CBTS) selection algorithm. In detail, both NBTS and CBTS exploit different types of antennas' control criteria and take into account several parameters: (i) the Global Navigation Satellite System (GNSS) *in-flight* coordinates of the UAV, gathered from the drone's FC telemetry; (ii) the flight direction of the UAV (also denoted as *heading angle* on a bidirectional plane); and (iii) the list of the cell towers of the ISP providing cellular connectivity, with their GNSS coordinates and cell IDs.

More in detail, once all the data are received, the NBTS algorithm *first* loads the known BTSs' GNSS location list, filtering them on the basis of the geographical distance between the drone and each BTS. *Then*, once the nearest BTS has been selected, the algorithm calculates the bearing angle between the UAV's GNSS coordinates and those of the selected nearest BTS. *Finally*, exploiting the UAV's heading angle and the bearing angle of the nearest BTS, the NBTS algorithm selects the antenna (out of the four antennas available on board the UAV) pointing towards the nearest BTS, leaving the others antennas disabled.

Instead, besides considering the same inputs of NBTS, the CBTS selection algorithm takes into account, as an additional parameter, the cell ID of the BTS which the cellular modem is connected to. Consequently, as for the NBTS, an *initial* temporary BTS selection is performed to consider only the closest BTSs and, once a cellular network connection has been established, the CBTS algorithm retrieves the LTE cell ID directly inspecting the network traffic. *Then*, the CBTS looks for the BTS identified by the same cell ID (inside the BTSs' list) and retrieves its GNSS coordinates, thus calculating the geographical distance and the bearing angle with respect to the UAV position. *Finally*, once the BTS of interest has been identified, using the drone's heading angle and the computed bearing angle of the selected cell tower it is possible to select the antenna pointing towards the BTS the UAV is connected to, while the other antennas

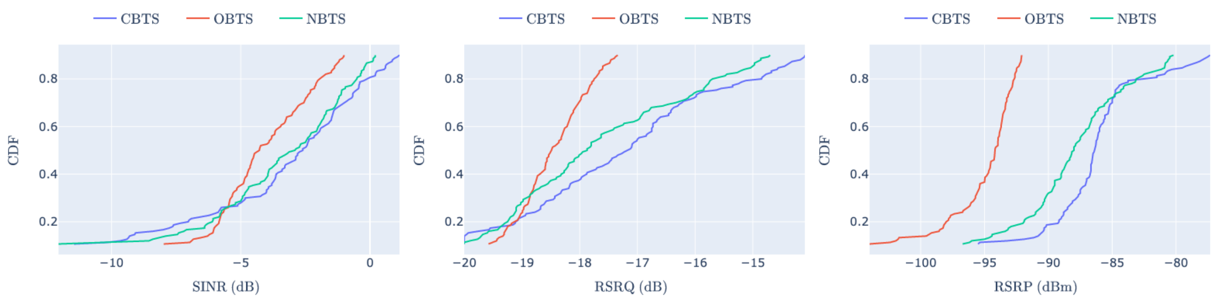

(a) (b) (c)

Figure 4: (a) CDF of the SINR, (b) CDF of the RSRQ, (c) CDF of the RSRP, all among the considered experimental setups (NBTS, CBTS, OBTS) at a 100 m AGL flight height.

are turned *off*.

As a final remark, both NBTS and CBTS algorithms reiterate every 500 ms: this value has been experimentally evaluated to make the proposed selective antenna mechanism efficient.

4. Experimental Results

In order to evaluate the performance of the proposed selective antenna system and to compare it with omni-directional antenna-based solutions, several automatic flights (scheduled to follow pre-defined flight paths) have been conducted to gather 4G LTE radio quality metrics with different antennas setups, namely (i) standard omni-directional antennas (denoted as OBTS) and (ii) selective antennas (detailed in Section 3) controlled through NBTS or CBTS algorithms. Then, in order to comply with the European Union Aviation Safety Agency (EASA) regulations [13], the experimental flights have been carried out in the Po Valley, near Sabbioneta, Italy, in a semi-rural area completely flat and without hills, featuring direct visibility for tens of BTSs within a few kilometer distance. This made the experimental area suitable for verifying the proposed solution, given the large number of nearby BTSs causing inter-cell interference at the flying drone. The experimental campaigns have been performed at low (20 m AGL) and high (100 m AGL) flight altitudes, evaluating (i) RSRP, RSRQ, and SINR metrics, and (ii) the number of cellular cell changes introduced in Section 2.

4.1. Radio Quality Metrics at Different Flight Heights

As a pre-processing operation, all the data collected at 20 m AGL and 100 m AGL have been properly "cleaned" removing data gathered during *take off* and *landing* phases. Then, data have been grouped according to the UAV's flight height, to perform a meaningful comparison between the three experimental system setups (namely: NBTS, CBTS, and OBTS). For the sake of clarity, in the following the SINR, RSRQ, and RSRP (defined in Section 2) will be investigated in terms of their Cumulative Distribution Functions (CDFs), to better compare and investigate gains and drawbacks of our proposed smart selective antenna system. We will also investigate the number of cell changes, which is another relevant metric to determine the network stability: the smaller the number of cell changes, the more reliable the connection link.

With regard to the drone flying at 100 m AGL, the corresponding CDFs of the SINR, RSRQ, and RSRP are shown in Figure 4(a), Figure 4(b), and Figure 4(c), respectively. In Table 1, the average values of SINR, RSRQ, and RSRP are shown at two representative heights: 20 m AGL and 100 m AGL (as considered in Figure 4).

Analyzing the results shown in Figure 4, one can observe, on average, an RSRP improvement when selective antennas are used—the average RSRP for the CBTS solution is more than 10 dBm

Table 1: SINR, RSRQ, and RSRP measurements obtained at the considered experimental flight heights (namely: 20 m AGL and 100 m AGL) with the different antennas setups.

Algorithm	20 m			100 m		
	SINR [dB]	RSRQ [dB]	RSRP [dBm]	SINR [dB]	RSRQ [dB]	RSRP [dBm]
CBTS	2.63	−13.85	−81.66	−1.45	−15.82	−84.20
NBTS	1.94	−13.99	−82.53	−1.97	−16.32	−85.85
OBTS	2.9	−15.43	−88.30	−2.62	−17.87	−94.33

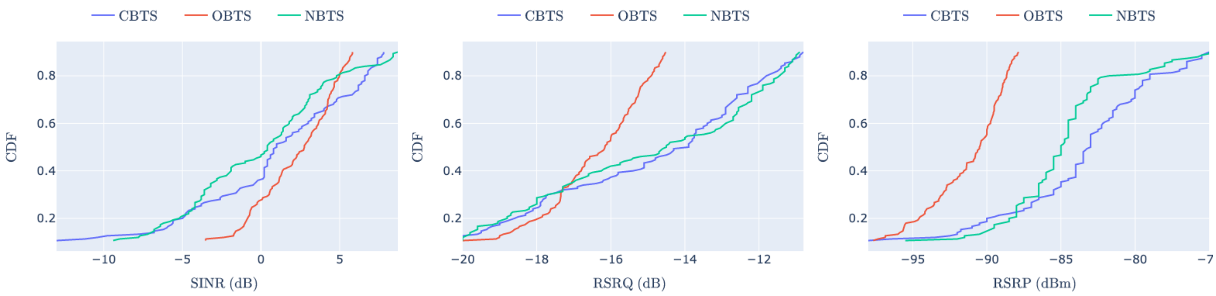

(a) (b) (c)

Figure 5: (a) CDF of the SINR, (b) CDF of the RSRQ, (c) CDF of the RSRP, all among the considered experimental setups (NBTS, CBTS, OBTS) at a 20 m AGL flight height.

higher than with omni-directional antennas, while the NBTS achieves a 8.5 dBm gain with respect to the OBTS. Regarding the average SINR, both CBTS and NBTS manage to achieve better values, with NBTS leading to an improvement around 0.6 dB and CBTS leading instead to a (higher) 1.2 dB gain. Finally, the same applies to RSRQ, with CBTS achieving a gain of almost 2 dB and NBTS of almost 1.5 dB. Overall, from a radio signal quality perspective, at 100 m AGL the best solution seems to be the adoption of a CBTS-controlled selective antenna mechanism since, on average, it returns better radio performance than NBTS.

Considering the scenario with the drone flying at 20 m AGL, the corresponding CDFs of the SINR, RSRQ, and RSRP are shown in Figure 5(a), Figure 5(b), and Figure 5(c). As anticipated before, the average values are listed in Table 1. Focusing on the results shown in Figure 5, it can be observed that the benefit of the proposed smart selective antenna system seems to be limited to RSRP and RSRQ values, while there is advantage, with respect to an omni-directional antenna-based system, in terms of SINR. In detail, RSRP gains are within 7 dBm (CBTS) and 6 dBm (NBTS) with the selective antenna system, with CBTS thus achieving the best performance. Finally, RSRQ returns similar values between CBTS and NBTS, both achieving an average gain closer to 1.5 dB with respect to the omni-directional solution.

4.2. Number of Cell Changes

According to the data collected during the experimental flights, the proposed selective antenna system experiences a smaller number of cell changes with respect to the omni-directional system, with NBTS experiencing, on average, 37.6 cell changes per flight, taking into account all the flights altitudes of the flight path. In comparison, CBTS experiences 46.2 cell changes per flight (on average), while the omni-directional antenna-based system experiences 54.3 cell changes per flight (on average). Therefore, it can be concluded that our proposed selective antenna system achieves better performance, especially if controlled through the CBTS algorithm allowing (especially at higher altitudes, where the drone is in LOS with most of the BTSs) to significantly decrease the inter-cell interference, thus improving the overall communication link stability.

5. Conclusions

In this paper, we have investigated experimental (and promising) results obtained comparing the adoption of standard (and traditional) omni-directional antennas with a prototypical smart selective antenna system controlled by innovative mechanisms (namely, NBTS and CBTS). The results show that the adoption of selective antennas (aiming at enhancing the cellular connectivity for UAV in BVLOS conditions) may be beneficial (as expected) at higher altitudes, where the inter-cell interference is significantly higher. In particular, our results show that the best control mechanism is CBTS, since, given the obstacle-free LOS path between the UAV and the BTSs, the different transmission power of the cells towers lead to achieve the best performance by enabling the antenna pointing towards the connected BTS instead of the closest one. Future research directions include the simultaneous use of our multiple antenna architecture together with a beamforming network, in order to compensate the weak antenna gain between two consecutive antennas disposed on two different sides. Such novel architecture might be beneficial at lower flight altitudes, where the performance of the current proposed prototype is worse than that with traditional omni-directional antennas. Finally, implementation aspects could be optimized, including the antenna form factor as well as the support for different frequency ranges.

Acknowledgments

This work received funding from the European Union's Horizon 2020 research and innovation program ECSEL Joint Undertaking (JU) under grant agreement No. 876019, ADACORSA project - "Airborne Data Collection on Resilient System Architectures". The JU received support from the European Union's Horizon 2020 research and innovation programme and the nations involved in the mentioned projects. The work reflects only the authors' views; the European Commission is not responsible for any use that may be made of the information it contains.

References

[1] Grand View Research, Inc Commercial Drone Market Size, Share & Trends Analysis Report `https://tinyurl.com/gwrdrones`.
[2] Parrot ANAFI Ai: The 4G robotic UAV `https://www.parrot.com/en/drones/anafi-ai`.
[3] Guckian P LTE Unmanned Aircraft Systems Trial Report `https://tinyurl.com/qcomuav`.
[4] Lin X *et al.* Mobile Network-Connected Drones: Field Trials, Simulations, and Design Insights *IEEE Vehicular Technology Magazine*, vol. 14, no. 3, pp. 115–125, 2019. doi:10.1109/MVT.2019.2917363.
[5] Zulkifley M A *et al.* Mobile Network Performance and Technical Feasibility of LTE-Powered Unmanned Aerial Vehicle *Sensors*, vol. 21, no. 8, 2021. doi:10.3390/s21082848.
[6] Fotouhi A *et al.* Survey on UAV Cellular Communications: Practical Aspects, Standardization Advancements, Regulation, and Security Challenges *IEEE Communications Surveys & Tutorials*, vol. 21, no. 4, pp. 3417–3442, 2019. doi:10.1109/COMST.2019.2906228
[7] European Telecommunications Standards Institute (ETSI) 2017 3GPP - 36.214 Evolved Universal Terrestrial Radio Access (E-UTRA); Physical layer - Measurements TS 36.214 `https://tinyurl.com/ETSITS136214`.
[8] Third Generation Partnership Project (3GPP) 2018 Enhanced LTE Support for Aerial Vehicles TR 36.777 `https://www.3gpp.org/ftp//Specs/archive/36_series/36.777/`.
[9] Muruganathan S D *et al.* An Overview of 3GPP Release-15 Study on Enhanced LTE Support for Connected Drones doi:10.48550/arXiv.1805.00826.
[10] Zhang S and Zhang R Radio Map-Based 3D Path Planning for Cellular-Connected UAV *IEEE Transactions on Wireless Communications*, vol. 20, no. 3, pp. 1975–1989, 2021. doi:10.1109/TWC.2020.3037916.
[11] Nguyen H C *et al.* How to Ensure Reliable Connectivity for Aerial Vehicles Over Cellular Networks *IEEE Access*, vol. 6, pp. 12304–12317, 2018. doi:10.1109/ACCESS.2018.2808998.
[12] Sierra Wireless EM9191 5G NR Sub-6 GHz Module `https://tinyurl.com/swem9191`.
[13] European Union Aviation Safety Agency (EASA) `https://www.easa.europa.eu/`.